

Quantum Chemical Study of Diels–Alder Reactions Catalyzed by Lewis Acid Activated Oxazaborolidines

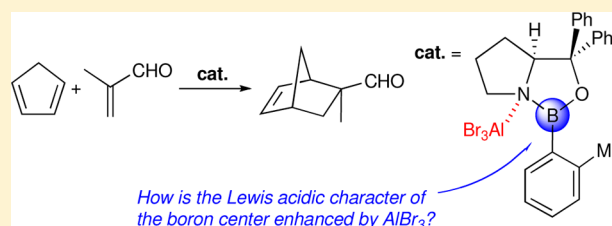
Ken Sakata^{*,†} and Hiroshi Fujimoto^{‡,§}

[†]Faculty of Pharmaceutical Sciences, Hoshi University, Ebara, Shinagawa-ku, Tokyo 142-8501, Japan

[‡]Department of Molecular Engineering, Graduate School of Engineering, Kyoto University, Katsura, Nishikyo-ku, Kyoto 615-8510, Japan

S Supporting Information

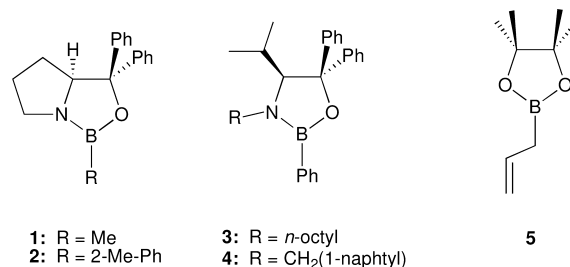
ABSTRACT: The catalytic activity of Lewis acid activated oxazaborolidines in the Diels–Alder reaction between cyclopentadiene and methacrolein is investigated by using the DFT method. Oxazaborolidine is not able to coordinate to methacrolein in the absence of AlBr_3 because the bonding stabilization is too small to cover the destabilization arising from the deformation of the two species. Accordingly, oxazaborolidine hardly catalyzes the cycloaddition by itself. The calculations show that the attachment of AlBr_3 to the nitrogen atom of oxazaborolidine enhances the Lewis acidity of its boron center and enables it to coordinate to methacrolein. When the AlBr_3 -assisted oxazaborolidine is once coordinated, the catalytic activity originates mainly from the oxazaborolidine framework, and to a smaller extent from the attached AlBr_3 part. The Lewis acid AlBr_3 plays an additional role to facilitate the reaction by reducing the overlap repulsion between the diene and the dienophile. The attachment of AlBr_3 to the oxygen atom, another Lewis basic site in oxazaborolidine, also gives a stable AlBr_3 –oxazaborolidine complex, but the reaction catalyzed by this complex is not preferred to that catalyzed by the complex in which AlBr_3 is attached to the nitrogen atom. The electrophilicity of boron center in oxazaborolidine and those in the AlBr_3 –oxazaborolidine complexes are compared in terms of localized reactive orbitals.



INTRODUCTION

Chiral oxazaborolidine (**1**), which has the Lewis acidic boron atom adjacent to the Lewis basic nitrogen atom, is a useful catalyst for the enantioselective reduction of ketones in the presence of BH_3 (Corey–Bakshi–Shibata (CBS) reduction).^{1–3} The initial key step of the reaction has been suggested to be the coordination of BH_3 to the nitrogen atom in **1**. Recently, protic and Lewis acid promoted chiral oxazaborolidines have been utilized as the catalyst for the enantioselective Diels–Alder reactions.^{4–15} Corey and co-workers developed the Diels–Alder reactions catalyzed by proline-derived oxazaborolidines with the protic acid, trifluoromethanesulfonic acid (TfOH) or trifluoromethanesulfonimide (Tf_2NH).^{4–9} They also reported that oxazaborolidine **2** shows a catalytic activity in the presence of the Lewis acid, AlBr_3 or BBr_3 .^{4,10,11} Yamamoto and co-workers showed that the combination of valine-derived oxazaborolidine (**3** or **4**) and Lewis acids such as SnCl_4 gives effective catalysts for the enantioselective Diels–Alder reactions.¹² They also reported that pentafluorophenylbis(trifluoromethanesulfonyl)methane ($\text{C}_6\text{F}_5\text{CHTf}_2$) activates **4**.^{13,14}

As in the CBS reduction, the Lewis acidic boron center in oxazaborolidine is assumed to be activated by the attachment of protic or Lewis acid to the adjacent nitrogen atom in the enantioselective Diels–Alder reactions. Therefore, these oxazaborolidines are classified into the Brønsted or Lewis acid assisted Lewis acids (BLA or LLA) with the concept of the



combined acid catalysis proposed by Yamamoto.¹⁶ In pinacol allylboronate (**5**), on the other hand, the Lewis acid attached to one of the oxygen atoms has been shown to enhance the Lewis acidity of the boron center.¹⁷ Our theoretical analysis has demonstrated that the electrophilicity of the boron center is strengthened not by charge shift from **5** to the attached Lewis acid as supposed but mainly by charge polarization in the B–O bond induced by the positive charge on the boron or aluminum center of the attached Lewis acid, BF_3 or AlCl_3 .¹⁸ It is also interesting to see why a Lewis acid is assumed a priori to attach not to the oxygen but to the nitrogen of oxazaborolidine.

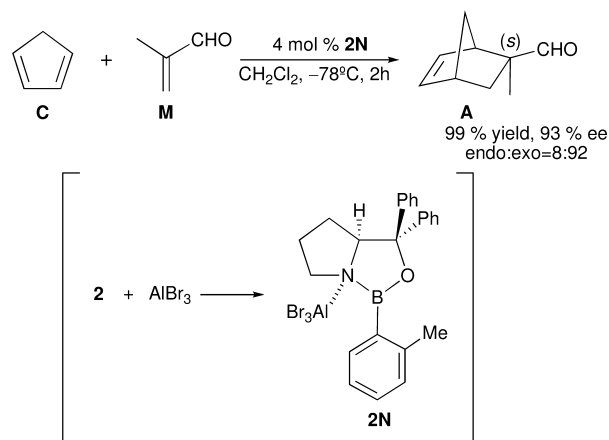
These catalytic systems have been investigated experimentally and theoretically primarily from the enantioselectivity point of view. The Diels–Alder reaction catalyzed by the

Received: January 12, 2013

Published: February 1, 2013

protonated cationic oxazaborolidine was studied theoretically by Pi and Li employing a simple model reaction system.¹⁹ More recently, Paddon-Row and co-workers examined in detail the cationic oxazaborolidine-catalyzed Diels–Alder reactions by using DFT calculations and showed that the obtained results reproduce the experimental enantioselectivity.^{20,21} Zain and co-workers also examined the enantioselectivity and mechanism of Diels–Alder reactions catalyzed by chiral cationic oxazaborolidines.²² The bulkiness of reagent and reactant that brings certain atoms or groups to a close proximity at the transition state controls the selectivity in many cases.²³ The repulsive interaction between the reagent and reactant may be imagined by looking at their three-dimensional geometries and is estimated by calculating the overlap repulsion or exchange repulsion in the DFT and MO theoretical calculations.²⁴ It is important, however, to design novel catalytic systems to know how and why such boron compounds, e.g., **2**, are assisted by the added Lewis acid, e.g., AlBr₃. We attempt in this study to disclose the electronic mechanism of the enhanced Lewis acidity of oxazaborolidine caused by an attachment of AlBr₃ in the Diels–Alder reaction between cyclopentadiene and methacrolein. The reaction catalyzed by an AlBr₃–oxazaborolidine complex (**2N**) reported by Corey and co-workers (Scheme 1)¹⁰ is studied by deriving the reactive orbitals that are localized on the reaction sites of the diene and dienophile parts.

Scheme 1. Diels–Alder Reaction Reported by Corey and Co-workers¹⁰



COMPUTATIONAL DETAILS

The quantum chemical calculations were carried out with the Gaussian03,^{25a} Gaussian09,^{25b} and GAMESS²⁶ program packages. Geometry optimization and analytical vibrational frequency analysis were performed by the B1B95 Kohn–Sham DFT method^{27–29} with the 6-31G* basis sets³⁰ (B1B95/6-31G*). The energies of each structure were calculated also by using the M06-2X DFT method^{31,29} and ab initio MP2 method with the 6-311G* basis set^{30a} (M06-2X/6-311G**/B1B95/6-31G* and MP2/6-311G**/B1B95/6-31G*).³²

RESULTS AND DISCUSSION

Transition-State Models. We explored 64 transition-state structures for the *exo* or *endo* attack of cyclopentadiene (**C**) to methacrolein (**M**) catalyzed by AlBr₃–oxazaborolidine complex **2N** at the M06-2X/6-311G**/B1B95/6-31G* level of theory (see the Supporting Information). In these structures, one of the oxygen lone pairs of electrons in *s-trans* or *s-cis* methacrolein is coordinated by the boron atom of **2** in the convex face.²¹

Among these transition-state structures, **TS-6XCR**, which is brought about by the *exo* attack to the *s-cis* form of **M** and leads to the minor product (**R**) in experiments, has the lowest Gibbs free energy at 195K (see the Supporting Information). In **TS-6XCR**, **M** is coordinated by **2N** and a hydrogen atom of **M** interacts with the oxygen atom in **2**, the C–H⋯O distance being 2.381 Å, as shown in Figure 1. The transition-state model proposed by Corey for the *exo* attack of **C** to the *s-trans* form of **M** to give the major product (**S**) corresponds to **TS-1XTS** or **TS-6XTS**. These structures allow the C–H⋯O interaction with the H⋯O distance of 2.336 Å in **TS-1XTS** and 2.352 Å in **TS-6XTS**, but the Gibbs free energy at 195 K is higher both in **TS-1XTS** and in **TS-6XTS** than in **TS-6XCR** by 6.0 and 5.1 kcal/mol, respectively. The structure, **TS-8XCS**, in which **M** in the *s-cis* form is coordinated by **2N**, has been shown to be the lowest in Gibbs free energy among the transition states that afford the major product (**S**) in experiments. While the Gibbs free energy is calculated to be higher in **TS-8XCS** than in **TS-6XCR** by 1.4 and 0.2 kcal/mol at the M06-2X/6-311G**/B1B95/6-31G* and MP2/6-311G**/B1B95/6-31G* levels, respectively, the former is located lower than the latter by 0.5 kcal/mol at the MP2/6-311G**/M06-2X/6-311G* level.³³ There might be some other factors that do not appear in the present calculations, but it is strongly suggested that **TS-8XCS** in which the C–H⋯O interaction is absent plays a crucial role in determining the enantioselectivity of the cycloaddition reactions catalyzed by the Lewis acid activated oxazaborolidine. This makes a clear contrast to the reaction catalyzed by the protonated oxazaborolidine cation. The transition-state structure which corresponds to **TS-1XTS** proposed by Corey is calculated to be lower in Gibbs free energy than the structures that correspond to **TS-6XCR**, **TS-6XTS**, and **TS-8XCS** by 5.4, 5.1, and 6.4 kcal/mol, respectively, at the MP2/6-311G**/B1B95/6-31G* level in the protonated oxazaborolidine case³⁴ (see the Supporting Information).

In **TS-8XCS**, the bond being formed between C¹(**C**) and C³(**M**) is 2.216 Å and that being formed between C⁴(**C**) and C²(**M**) is 2.978 Å at the B1B95/6-31G* level of theory. The change in bond lengths along the IRC³⁵ is shown in Figure 2. This IRC connects the transition state **TS-8XCS** to the reactant complex **RC-8XCS** (*s* < 0) and to the product complex **PR-8XCS** (*s* > 0). In **RC-8XCS**, the C–C bonds are not yet formed, the C¹(**C**)–C³(**M**) and C⁴(**C**)–C²(**M**) distances being 3.033 and 3.207 Å, respectively. The geometry of **RC-8XCS** looks like a π-type complex between the diene moiety of **C** and the vinyl group of **M** (see the Supporting Information). As shown in Figure 2, the formation of the C¹–C³ bond precedes that of the C⁴–C² bond throughout the course of the reaction. The cycloaddition is concerted but not synchronous, in line with the results of theoretical calculations on the cycloaddition reactions of α,β-unsaturated aldehydes with dienes catalyzed by a variety of Lewis acids.^{19,20,22,36,37}

Energy Diagrams. In the case of the reaction path via **TS-8XCS**, the coordination of the AlBr₃–oxazaborolidine complex **2N** to *s-cis* methacrolein affords the complex **CX-8** as shown in Figure 3. In **CX-8**, the B–O(**M**) bond length is 1.639 Å and the B–C(*o*-tolyl group) bond and the methacrolein framework are placed approximately within a plane, and accordingly, the C–H(**M**)⋯O(**2N**) interaction is not feasible. The free energy difference accompanied by the complexation is calculated to be -1.6 kcal/mol at the M06-2X/6-311G**/B1B95/6-31G* level of theory. Then, the *exo* attack of **C** to **CX-8** gives a reactant complex **RC-8XCS**, which leads to the transition state **TS-**

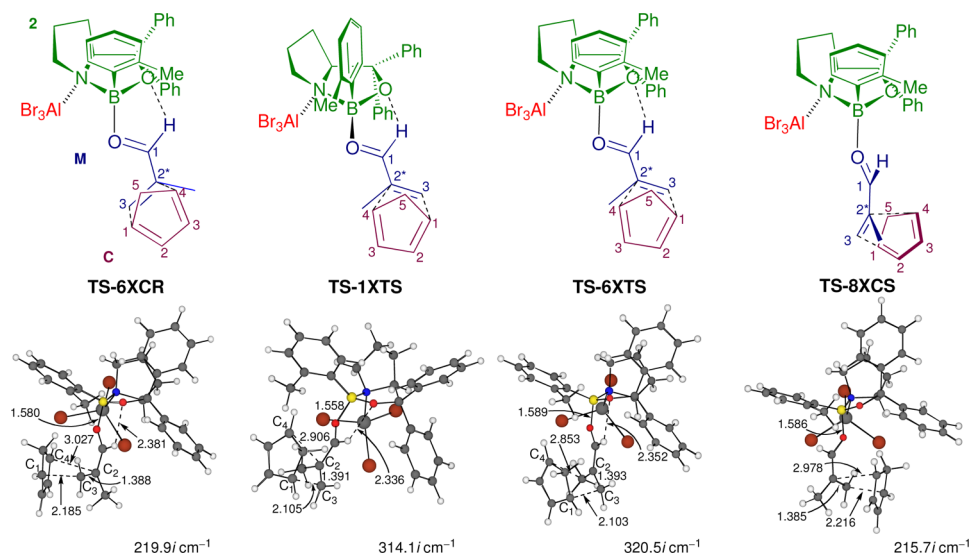


Figure 1. Transition-state structures TS-6XCR, TS-1XTS, TS-6XTS, and TS-8XCS optimized at the B1B95/6-31G* level.

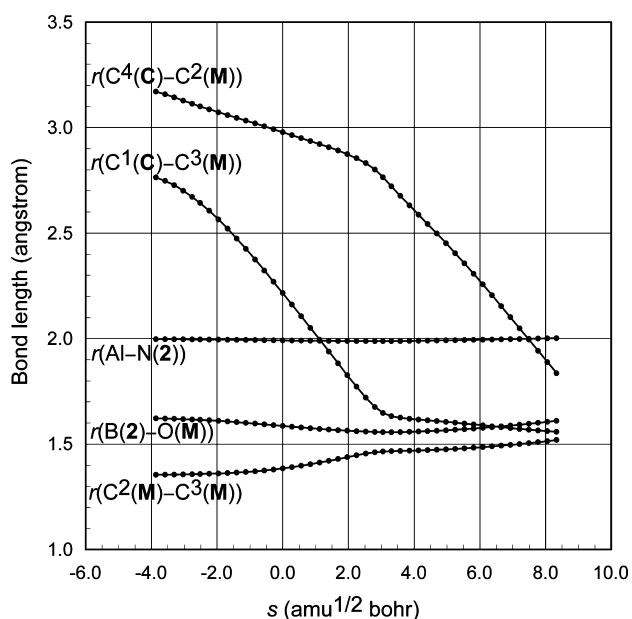


Figure 2. Change in the bond lengths along IRC of TS-8XCS.

8XCS. The change in free energy relative to the initial state, (C + M(*s-trans*) + 2N) without interaction, is 3.2 kcal/mol at TS-8XCS. This transition state leads then to the product PR-8XCS which is a complex between the cycloadduct A1 and 2N. The dissociation of TS-8XCS to free A1 from the catalyst 2N costs 4.6 kcal/mol in free energy.

The AlBr₃ molecule detached from 2N may coordinate to a methacrolein molecule to give an AlBr₃-coordinated *s-trans* methacrolein (M⋯AlBr₃). The free energy relative to the state, (M(*s-trans*) + 2N) without interaction, is -1.2 kcal/mol at the state (M⋯AlBr₃ + 2). Then, the attack of C into the AlBr₃-coordinated methacrolein provides the cycloaddition directly catalyzed by AlBr₃. The transition state for the *endo* attack of cyclopentadiene into the AlBr₃-coordinated *s-cis* methacrolein (TS' in Figure 3),^{38,39} is located slightly higher, 4.3 kcal/mol, than the transition state TS-8XCS, 3.2 kcal/mol. This indicates that the reaction catalyzed by 2N should be preferred to the reaction directly catalyzed by AlBr₃ at a lower temperature. This

is in agreement with the experimental observation that excess amount of Lewis acid does not affect the enantioselectivity in the cycloadditions.¹²

For comparison, we examined also the cycloaddition without any catalyst and the reaction catalyzed by oxazaborolidine without an assistance of AlBr₃, as shown in Figure 3. The free energy of the transition state for the former case, the *exo* attack of C into the *s-cis* methacrolein (TS), is as high as 20.9 kcal/mol at the M06-2X/6-311G**/B1B95/6-31G* level.⁴⁰ On the other hand, the calculations at the B1B95/6-31G* level of theory showed that 2 did not coordinate by itself to M to give a complex M⋯2, the bonding stabilization being too small to cover the destabilization arising from the deformation of the two species.⁴¹ We found, however, the transition-state structure (TS'') for the cycloaddition with C in which the distance between the boron atom in 2 and the oxygen atom in M is 1.727 Å (see the Supporting Information). It appears that electron delocalization from C to M in the reaction has strengthened the ability of the methacrolein moiety for electron donation to 2. The relative free energy of TS'' is 47.8 kcal/mol. This indicates that oxazaborolidine 2 hardly catalyzes the cycloaddition by itself.

To see the effects of AlBr₃ on the interactions between diene and dienophile at the transition states, we performed a fragment analysis (see the Supporting Information). The interaction energy INT[C-(M·2·AlBr₃)] between the dienophile fragment with the Lewis acid assisted oxazaborolidine, (M·2·AlBr₃), and the C fragment is defined here by the energy difference between TS-8XCS and the two fragments each frozen to the same geometries that they have in the TS-8XCS structure. It is -16.0 kcal/mol at the B1B95/6-31G* level of theory. When AlBr₃ is removed from the (M·2·AlBr₃) fragment freezing the geometry of the remaining part, the interaction energy between the (M·2) fragment and the C fragment, INT[C-(M·2)], is reduced to -11.6 kcal/mol. The interaction energy between the dienophile fragment and the diene fragment, INT[C-M], is reduced further to -2.9 kcal/mol in the absence of 2. That is, the interaction between C and M is strengthened largely by the coordination of 2 to the latter and is further strengthened by the attachment of AlBr₃ to 2. It is important, first of all, to make 2 be able to coordinate to M by the aid of a Lewis acid, e.g., AlBr₃, but once (2·Lewis acid) has

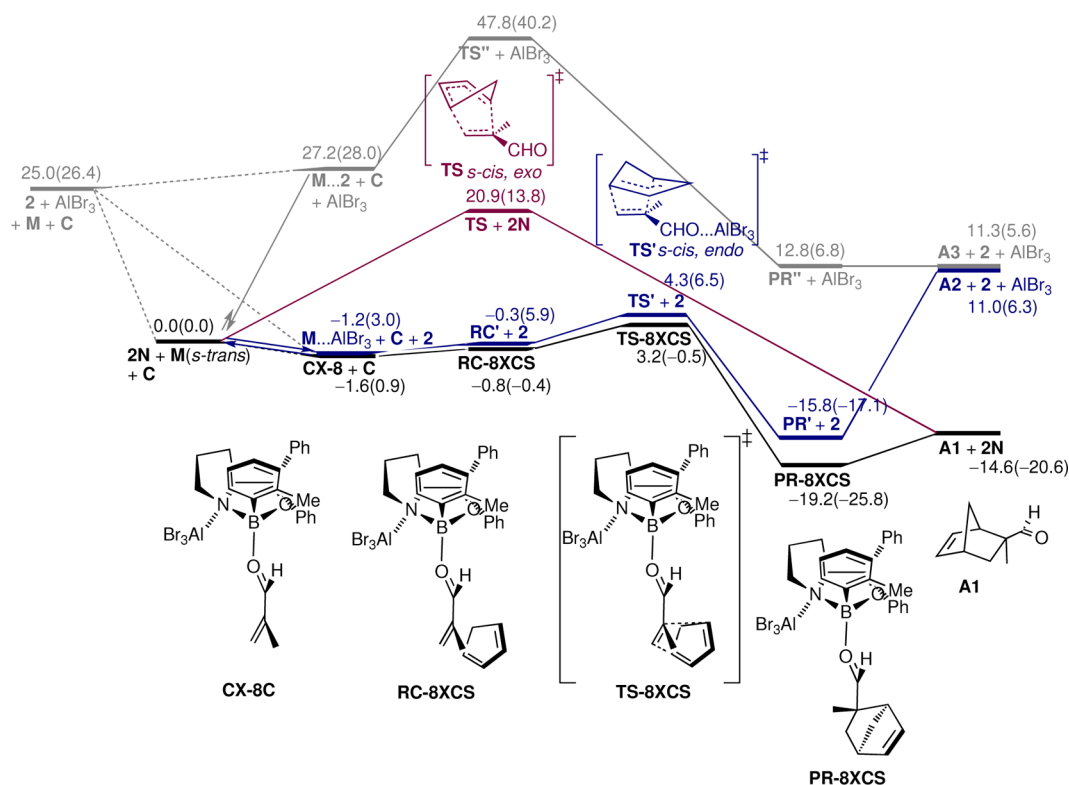
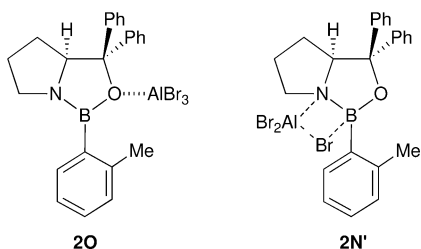


Figure 3. Gibbs free energy diagram at a temperature of 195 K at M06-2X/6-311G*//B1B95/6-31G* level of theory (kcal/mol). Relative free energies at MP2/6-311G*//B1B95/6-31G* level of theory are in parentheses. See ref 41 for a weak complex $M \cdots 2$ between **2** and *s-trans* methacrolein.

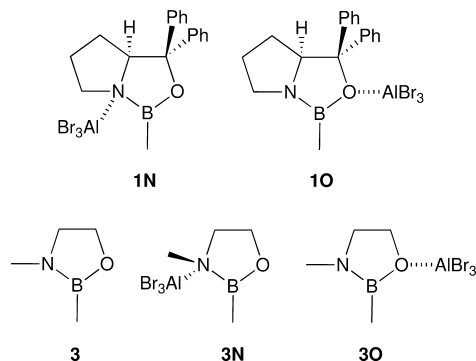
been coordinated, the acceleration of the reaction is brought about primarily by **2**.

Coordination of $AlBr_3$ to the Oxygen Atom at Oxazaborolidine. Oxazaborolidine **2** has another Lewis basic site, the oxygen atom, although it has scarcely been regarded as the coordination site in the literature. We examine here the catalytic activity of the $AlBr_3$ –oxazaborolidine complex **2O**, where $AlBr_3$ coordinates to the oxygen atom of **2**, in the cycloaddition reactions.



The energies of the $AlBr_3$ –oxazaborolidine complexes, **2N** and **2O**, relative to the state ($2 + AlBr_3$), ΔE , are -36.6 and -33.3 kcal/mol, respectively, at the M06-2X/6-311G*//B1B95/6-31G* level of theory. The complex **2N** is more stable than **2O**, but the energy difference, 3.3 kcal/mol, is not so large. In the case of protonated oxazaborolidine, the N-protonated complex which corresponds to **2N** is far more stable, by up to 20.5 kcal/mol, than the O-protonated complex which corresponds to **2O**. The bridged structure **2N'**, in which one of the bromine atoms is shared by the boron atom in oxazaborolidine and aluminum atom in $AlBr_3$,⁴² was not found in the present system. The fragment analysis at the B1B95/6-31G* level theory shows that INT in **2O**, -55.1 kcal/mol, is

smaller than that of **2N**, -65.2 kcal/mol, whereas the energy associated with the deformation, DEF, of **2O**, $+20.4$ kcal/mol, is smaller than that of **2N**, $+25.8$ kcal/mol. In $AlBr_3$ –oxazaborolidine complexes between $AlBr_3$ and unsubstituted oxazaborolidine **1**, the energy of the complex **1N** relative to the state ($1 + AlBr_3$), ΔE , is -39.8 kcal/mol, whereas ΔE is smaller, -35.6 kcal/mol, in the complex **1O** at the M06-2X/6-311G*//B1B95/6-31G* level of theory. In contrast, the complex **3O**, $\Delta E = -39.3$ kcal/mol, is calculated to be more stable than the complex **3N**, $\Delta E = -36.6$ kcal/mol, in the complexes with a simple oxazaborolidine model, **3**.⁴³ The stability of these complexes is determined by a balance between the structural deformation and the Lewis acidity of the coordination site. Except for the case of protonated oxazaborolidine, the oxygen atom may be regarded as another coordination site of Lewis acids.



We thus examined three transition-state structures **TS-O1**, **TS-O2**, and **TS-O3** shown in Figure 4 for the cycloaddition

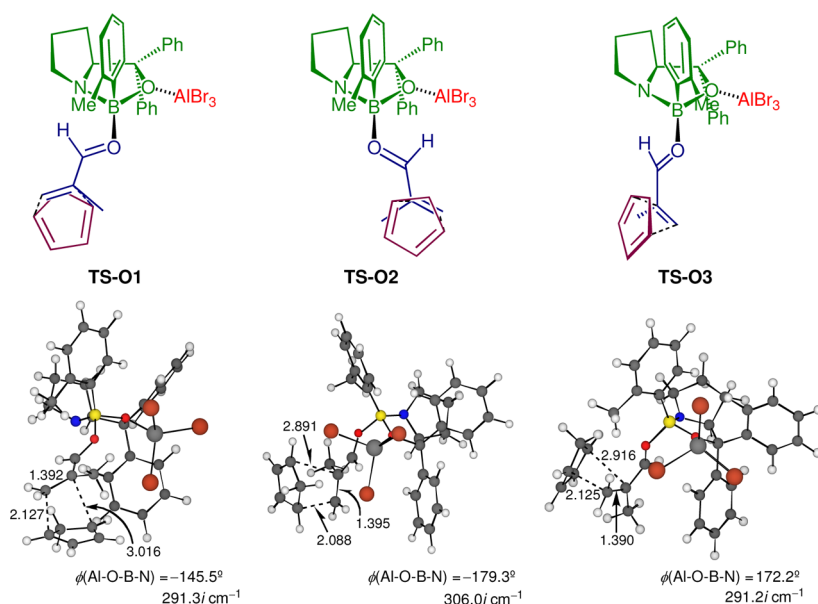


Figure 4. Transition-state structures TS-O1, TS-O2, and TS-O3 optimized at the B1B95/6-31G* level.

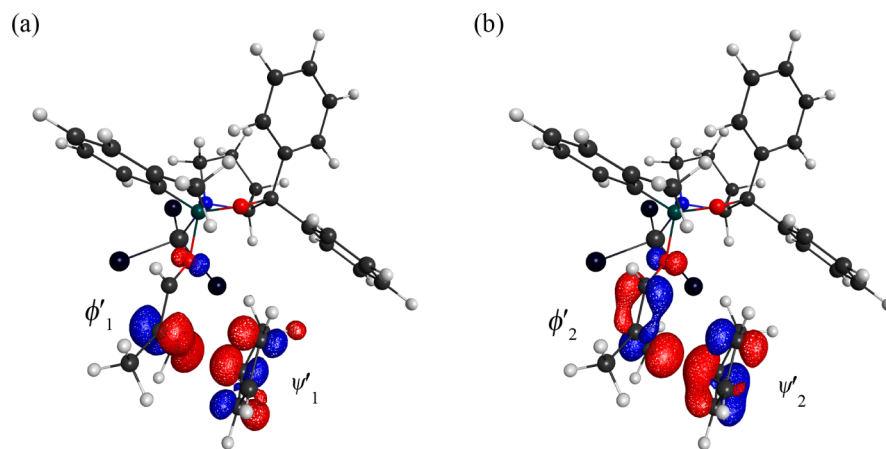


Figure 5. Pairs of interacting orbitals of TS-8XCS (ψ'_1 ; ϕ'_1) and (ψ'_2 ; ϕ'_2), calculated at the B1B95/6-31G* level of theory.

reaction catalyzed by the complex **20**. The calculations show, however, that the free energies of TS-O1, TS-O2, and TS-O3 relative to the initial state (**C** + **M**(*s-trans*) + **2N**) are 21.5, 21.7, and 25.7 kcal/mol, respectively, at the M06-2X/6-311G**/B1B95/6-31G* level of theory. They are much higher than that of TS-8XCS, 3.2 kcal/mol. This result suggests that the reaction catalyzed by **20** is unlikely.

Electron Population and Orbital Interactions. An analysis using the interaction frontier orbitals (IFOs)⁴⁴ shows that electron delocalization from the (**M**·**2**·AlBr₃) fragment to the **C** fragment at TS-8XCS is characterized by a pair of orbitals (ψ'_1 ; ϕ'_1) as illustrated in part a of Figure 5. The orbital ψ'_1 consists of the unoccupied π -type Kohn–Sham orbitals of cyclopentadiene. It looks like the lowest unoccupied orbital of butadiene. The orbital ϕ'_1 is the π bonding orbital localized on the C=C bond of **M**, given by a linear combination of the occupied Kohn–Sham one-electron orbitals of the (**M**·**2**·AlBr₃) fragment. The orbitals ϕ'_1 and ψ'_1 are located at -9.09 eV and $+0.53$ eV in energy, respectively. Electron delocalization from **C** to (**M**·**2**·AlBr₃) is governed by a pair of orbitals (ψ'_2 ; ϕ'_2), illustrated in part b of Figure 5. The orbital ψ'_2 is the occupied π -like orbital of **C** having a large amplitude on C¹, and the

orbital ϕ'_2 is the π -type unoccupied orbital of (**M**·**2**·AlBr₃) having a large amplitude on C³. The orbital ψ'_2 is placed at -6.06 eV and ϕ'_2 at -3.22 eV. The unoccupied interacting orbital ϕ'_2 localized on the methacrolein skeleton is considerably low in energy, showing its enhanced ability of electron acceptance brought about by the coordination of AlBr₃-activated oxazaborolidine. The formation of the C¹(C)–C³(**M**) bond is facilitated.

The changes in the atomic net charges of **C**, **M**, **2**, and AlBr₃ parts estimated by the natural population analysis⁴⁵ along the IRC of TS-8XCS⁴⁶ show that the sum of the atomic net charges in **C** increases to positive while that in **M** decreases in positive in the vicinity of the transition state, where the C¹(C)–C³(**M**) bond is formed (see the Supporting Information). This indicates that electron delocalization from the diene part to the dienophile part, described by the orbital pair (ψ'_2 ; ϕ'_2), is stronger than electron delocalization from the latter to the former, as is often the case in the Diels–Alder reactions.⁴⁷ The electron-accepting ability of methacrolein enhanced by the attached AlBr₃-activated oxazaborolidine is obviously one of the reasons of this result. In the later stage of the reaction ($s > 2.0$ amu^{1/2} bohr), the sum of the atomic net charges in **M** increases

in positive, while that in C decreases. Electron delocalization from the dienophile part to the diene part, represented by the orbital pair (ψ'_1 ; ϕ'_1), takes place significantly to generate the $C^4(C)-C^2(M)$ bond and to strengthen further the $C^1(C)-C^3(M)$ bond. It is noted here that some fractions of electron population are retained not only by **2** but also by $AlBr_3$ throughout the course of the reaction. The calculations tell us that the electron population of C^3 is reduced significantly in **M** by the coordination of **2** onto the carbonyl oxygen and further by the attachment of $AlBr_3$ to **2**.⁴⁸ This must be the major origin of enhanced electron-accepting ability of **M** particularly on C^3 , as described above in the interaction orbital ϕ'_2 . The decrease in electron population on C and M leads concurrently to a mitigation of overlap repulsion, as indicated clearly in the sum of overlap populations coming from the antibonding interactions between the occupied orbitals of the diene and dienophile parts.⁴⁹ This should be another important role of the Lewis acid catalysts in the Diels–Alder cycloadditions, and the preceded formation of the $C^1(C)-C^3(M)$ bond is thus reasoned. A stronger Lewis acid should make the cycloaddition more asynchronous, as has been indicated in these calculations.^{36k}

When $AlBr_3$ is removed with the geometry of the remaining atoms frozen to the same as that in **TS-8XCS**, two pairs of orbitals are obtained that look very much the same as those obtained above for the interaction in the presence of $AlBr_3$ (see the Supporting Information). This means that the electronic mechanism of interaction between the two fragments is not altered in nature by the presence of $AlBr_3$. The electron-donating and -accepting orbitals in the (M·2) fragment, ϕ'_1 and ϕ'_2 , are elevated, however, by 0.22 and 0.33 eV in energy, respectively, compared with those in Figure 5. This indicates that the electron-accepting ability of **M** is weakened, while electron-donating ability is enhanced, though not large in magnitude, by removing $AlBr_3$ from the reacting system. These orbitals, ϕ'_1 and ϕ'_2 , are further elevated, by 1.05 eV and by 1.34 eV, when **2** is removed. The electron-accepting ability of **M** has been weakened significantly in this case. Orbital interactions show again that it is of crucial importance to make **2** be able to coordinate to **M** by the aid of a Lewis acid. Once it is coordinated, the strengthening of electron delocalization from C to the methacrolein moiety is brought about primarily by **2**. The Lewis acid $AlBr_3$ promotes further electron delocalization from C to **M**, but to a lesser extent. This is also shown clearly in the overlap population of the $C^1(C)-C^3(M)$ bond.⁵⁰ The present calculation suggests that the strengthening of the $C^1(C)-C^3(M)$ bond by **2** and/or by **2N** is attributed around half, 56–57%, to the strengthened electrophilicity of C^3 , and half, 43–44%, to the reduced overlap repulsion at **TS-8XCS**.⁴⁹ The use of Lewis acids having groups with strongly electron-holding capacity is recommended.

Electron delocalization from **M** to (2· $AlBr_3$) within the (M·2· $AlBr_3$) fragment having the same structure as that in **TS-8XCS** is represented by a pair of orbitals (ϕ'_3 ; ϕ'_3), which is shown in part a of Figure 6. These orbitals are located in energy at –9.09 and +0.97 eV, respectively. On the other hand, electron delocalization from **M** to **2** in the absence of $AlBr_3$ is represented by a pair of orbitals (ϕ''_3 ; ϕ''_3), illustrated in part b of Figure 6. The orbital pairs look very similar, but the orbital ϕ''_3 is higher in energy by 1.62 eV than ϕ'_3 . The electron-accepting level of the boron center has been lowered significantly by the attachment of $AlBr_3$ to the nitrogen atom without changing the mode of coordination of **2** to **M**.

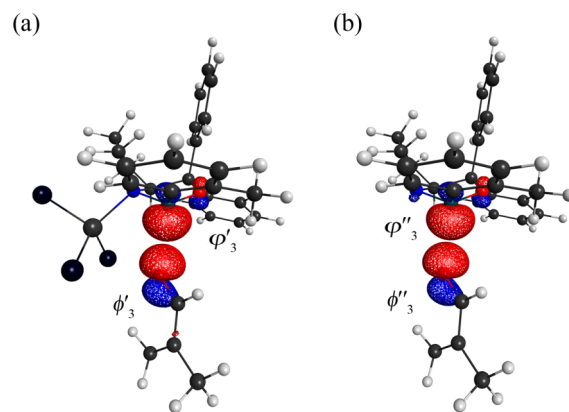


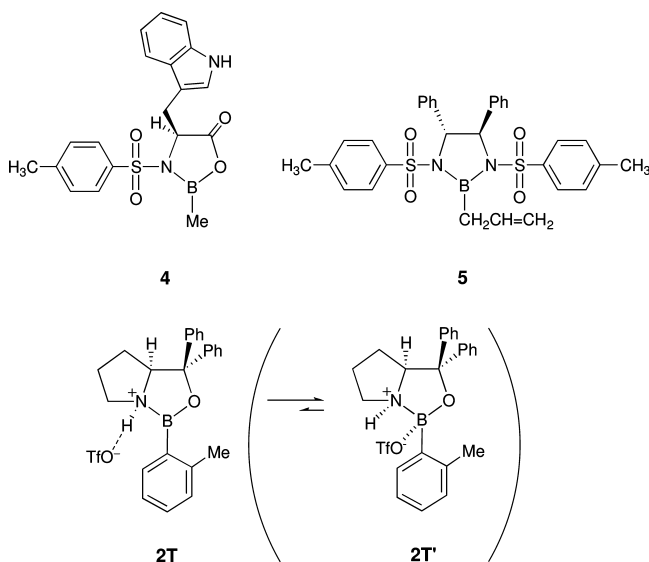
Figure 6. Pairs of interacting orbitals (ϕ'_3 ; ϕ'_3) within the (M·2· $AlBr_3$) fragment and (ϕ''_3 ; ϕ''_3) within the (M·2) fragment calculated at the B1B95/6-31G* level of theory.

In addition to the interaction represented by a pair of orbitals (ϕ'_3 ; ϕ'_3), there are weak interactions between one of the Br atoms of $AlBr_3$ and a π^* orbital of **M** and between another Br atom and a $C^3(M)-H$ σ^* orbital of **M** in **TS-8XCS**. There appears also an interaction between a Br atom and $C^3(M)-H$ σ^* orbital of **M** in **TS-6XCR**.⁵¹ The shortest Br–H distance is 2.580 Å in **TS-8XCS** and 2.696 Å in **TS-6XCR**. While the transition state in the system catalyzed by the protonated oxazaborolidine cation is stabilized mainly by the C–H···O interaction⁵² and by electron donation from the B–C(*o*-tolyl) σ orbital to the π^* orbitals of **M**, the bonding interactions between the bromine atoms in $AlBr_3$ with the π^* orbital in **M** and with the hydrogen atom on C^3 in **M** controls the stable conformation of the system catalyzed by $AlBr_3$ –oxazaborolidine complex.

Electrophilicity of the Boron Center in Oxazaborolidines. The electronic charge that is transferred to $AlBr_3$ is held by three bromine atoms, keeping the aluminum center charged positive, as in the case of $AlCl_3$ -attached pinacol allylboronate.¹⁸ The boron center in **2** is activated by the same mechanism as in the allylboronate, i.e., by means of induced polarization of the B–N bond in the field of a positive net charge on Al.¹⁸ Based on the above results, we examine how the Lewis acidic character on the boron atom in **2** is enhanced by the Lewis acid $AlBr_3$. In electron delocalization from methacrolein to the smallest boron compound BH_3 , the lowest unoccupied orbital has been shown to play an exclusive role in the BH_3 part. The LUMO of BH_3 is located at –1.45 eV at the B1B95/6-31G* level in an isolated state. In oxazaborolidines, the boron atomic orbitals are distributed over a number of Kohn–Sham orbitals. We projected then the boron components in the LUMO of BH_3 , δ_r , onto the unoccupied orbital space of **2**,^{18,53,54} to generate the orbital that is closest in character to the LUMO of BH_3 . The orbital of **2** has the energy expectation value, $\lambda_{unoc}(\delta_r)$, of +2.84 eV. The boron center in **2** has an electron-accepting ability considerably weaker than that in BH_3 . On the other hand, the $\lambda_{unoc}(\delta_r)$ of the $AlBr_3$ –oxazaborolidine complexes, **2N** and **2O**, are calculated to be +1.27 and +1.69 eV, respectively, which are lowered considerably compared with that of **2**. This signifies that the Lewis acidic character of the boron center is enhanced by the attachment of $AlBr_3$ to **2** and that the boron center in **2N** is more acidic than that in **2O**. These results obtained for the acids in an isolated state are reflected nicely in the barrier

heights calculated above and in the IFOs for the reacting systems.

We evaluated then the electrophilicity of the boron atom in the Lewis acid catalysts, **4** and **5**, which were used for the enantioselective Diels–Alder and allylation reactions.^{55,56} Wong examined theoretically the structure of a complex between 2-bromoacrolein and **4**, and suggested the importance of the C–H···O interaction and the π – π stacking.⁵⁷ In the obtained structure, the B–O bond distance is 1.65 Å,⁵⁷ which shows the definite dative bond structure. The $\lambda_{\text{unoc}}(\delta_r)$ values of **4** and **5** are +1.77 and +1.79 eV, respectively, suggesting that these catalysts are similar to, or slightly weaker than, **2N** in electrophilicity. The $\lambda_{\text{unoc}}(\delta_r)$ value of the complex **2T** which corresponds to the protic acid activated oxazaborolidine is calculated to be +0.71 eV, which is lower than that in **2N**. The catalytic activity of **2T** should be somewhat stronger than **2N** so far the electrophilicity of the boron atom is concerned. The counterion TfO[−] may prevent methacrolein from coordination in this case, by filling the boron site by itself (**2T'**).^{42,58} The efficiency in the catalytic cycle is another problem to be examined.



CONCLUSION

We have examined the Diels–Alder reaction between cyclopentadiene and methacrolein catalyzed by AlBr₃–oxazaborolidine complexes applying the DFT method. We located the transition-state structures, each leading to the major or minor products experimentally reported by Corey and co-workers. It was found that the C–H···O interaction does not play a crucial role in the cycloaddition catalyzed by the AlBr₃–oxazaborolidine complexes. The calculations showed that it is hard for oxazaborolidine to coordinate by itself to methacrolein, because the deformation associated with the coordination heavily destabilizes the system. The attachment of AlBr₃ strengthens the Lewis acidity of boron center in oxazaborolidine by polarizing the B–N bond in the field of a positive charge on Al to make the center more electron-deficient. Coordination of AlBr₃–oxazaborolidine enhances the electron-accepting ability of methacrolein, providing a low-lying unoccupied interaction orbital that has large amplitude on C³. Very interestingly, the calculations revealed that the acceleration of the Diels–Alder reaction is brought about mainly from the oxazaborolidine

framework, once it is coordinated, and, to a lesser extent, from the attached AlBr₃ part. Not only oxazaborolidine but also AlBr₃ keep fractions of electron population of the reactants within them throughout the course of reaction to reach the product stage. The fractions of electron population shifted are held on the nitrogen and bromine atoms. Thus, oxazaborolidine and the attached AlBr₃ play another important role to lessen the exchange or overlap repulsion between the reaction sites in the cycloaddition. The enhanced electrophilicity and the reduced repulsive interaction particularly on C³ in methacrolein promote the formation of the bond between C³ and C¹ in cyclopentadiene, preceding the formation of the other C–C bond in the reaction. These two have been evaluated to have influences similar in strength on the C¹–C³ bond formation.

The attachment of AlBr₃ to the oxygen atom at oxazaborolidine gives another AlBr₃–oxazaborolidine complex, in contrast to the protonated oxazaborolidine case. The transition state for the reaction catalyzed by this complex was shown by the calculations to be energetically less preferred to that catalyzed by the complex in which AlBr₃ was attached to the nitrogen atom. Lewis acids that are used in experiments for enantioselective Diels–Alder reactions are suggested to have similar electrophilicity on the boron-center to that of AlBr₃–oxazaborolidine complex.

ASSOCIATED CONTENT

Supporting Information

Tables listing energies and geometries. This material is available free of charge via the Internet at <http://pubs.acs.org>.

AUTHOR INFORMATION

Corresponding Author

*E-mail: sakata@hoshi.ac.jp.

Notes

The authors declare no competing financial interest.

§H.F. is an Emeritus Professor.

ACKNOWLEDGMENTS

This work was supported by a Grant-in-Aid for Scientific Research on Innovative Areas “Advanced Molecular Transformations by Organocatalysts” from The Ministry of Education, Culture, Sports, Science and Technology (Japan) and by ACT-C from Japan Science and Technology Agency. Some of the calculations were made at the Research Center for Computational Science, Okazaki, Japan. K.S. is grateful to the Research Center for Computational Science for generous permission to use its computing facilities.

REFERENCES

- Corey, E. J.; Bakshi, R. K.; Shibata, S. *J. Am. Chem. Soc.* **1987**, *109*, 5551–5553.
- For a review, see: Corey, E. J.; Helal, C. J. *Angew. Chem., Int. Ed.* **1998**, *37*, 1986–2012.
- For theoretical studies, see: (a) Alagona, G.; Ghio, C.; Persico, M.; Tomasi, S. *J. Am. Chem. Soc.* **2003**, *125*, 10027–10039 and references therein. (b) Alagona, G.; Ghio, C.; Tomasi, S. *Theor. Chem. Acc.* **2004**, *111*, 287–302.
- For a review, see: Corey, E. J. *Angew. Chem., Int. Ed.* **2009**, *48*, 2100–2117.
- Corey, E. J.; Shibata, T.; Lee, T. W. *J. Am. Chem. Soc.* **2002**, *124*, 3808–3809.
- Ryu, D. H.; Lee, T. W.; Corey, E. J. *J. Am. Chem. Soc.* **2002**, *124*, 9992–9993.
- Ryu, D. H.; Corey, E. J. *J. Am. Chem. Soc.* **2003**, *125*, 6388–6390.

- (8) Ryu, D. H.; Zhou, G.; Corey, E. J. *J. Am. Chem. Soc.* **2004**, *126*, 4800–4802.
- (9) Zhou, G.; Hu, Q.-Y.; Corey, E. J. *Org. Lett.* **2003**, *5*, 3979–3982.
- (10) Liu, D.; Canales, E.; Corey, E. J. *J. Am. Chem. Soc.* **2007**, *129*, 1498–1499.
- (11) Mukherjee, S.; Corey, E. J. *Org. Lett.* **2010**, *12*, 632–635.
- (12) Futatsugi, K.; Yamamoto, H. *Angew. Chem., Int. Ed.* **2005**, *44*, 1484–1487.
- (13) Payette, J. N.; Yamamoto, H. *J. Am. Chem. Soc.* **2007**, *129*, 9536–9537.
- (14) Payette, J. N.; Yamamoto, H. *Angew. Chem., Int. Ed.* **2009**, *48*, 8060–8062.
- (15) Shibatomi, K.; Futatsugi, K.; Kobayashi, F.; Iwasa, S.; Yamamoto, H. *J. Am. Chem. Soc.* **2010**, *132*, S625–S627.
- (16) Yamamoto, H.; Futatsugi, K. *Angew. Chem., Int. Ed.* **2005**, *44*, 1924–1942.
- (17) Rauniyar, V.; Hall, D. G. *J. Am. Chem. Soc.* **2004**, *126*, 4518–4519.
- (18) Sakata, K.; Fujimoto, H. *J. Am. Chem. Soc.* **2008**, *130*, 12519–12526.
- (19) Pi, Z.; Li, S. J. *Phys. Chem. A* **2006**, *110*, 9225–9230.
- (20) Paddon-Row, M. N.; Kwan, L. C. H.; Willis, A. C.; Sherburn, M. S. *Angew. Chem., Int. Ed.* **2008**, *47*, 7013–7017.
- (21) Paddon-Row, M. N.; Anderson, C. D.; Houk, K. N. *J. Org. Chem.* **2009**, *74*, 861–868.
- (22) (a) Omar, N. Y. M.; Rahman, N. A.; Zain, S. M. *Bull. Chem. Soc. Jpn.* **2011**, *84*, 196–204. (b) Omar, N. Y. M.; Rahman, N. A.; Zain, S. M. *J. Comput. Chem.* **2011**, *32*, 1813–1823.
- (23) *Catalytic Asymmetric Synthesis*, 3rd ed.; Ojima, I., Ed.; Wiley: Hoboken, 2010.
- (24) Fujimoto, H.; Mizutani, Y.; Endo, J.; Jinbu, Y. *J. Org. Chem.* **1989**, *54*, 2568–2573.
- (25) (a) Frisch, M. J.; Trucks, G. W.; Schlegel, H. B.; Scuseria, G. E.; Robb, M. A.; Cheeseman, J. R.; Montgomery, J. A., Jr.; Vreven, T.; Kudin, K. N.; Burant, J. C.; Millam, J. M.; Iyengar, S. S.; Tomasi, J.; Barone, V.; Mennucci, B.; Cossi, M.; Scalmani, G.; Rega, N.; Petersson, G. A.; Nakatsuji, H.; Hada, M.; Ehara, M.; Toyota, K.; Fukuda, R.; Hasegawa, J.; Ishida, M.; Nakajima, T.; Honda, Y.; Kitao, O.; Nakai, H.; Klene, M.; Li, X.; Knox, J. E.; Hratchian, H. P.; Cross, J. B.; Bakken, V.; Adamo, C.; Jaramillo, J.; Gomperts, R.; Stratmann, R. E.; Yazyev, O.; Austin, A. J.; Cammi, R.; Pomelli, C.; Ochterski, J. W.; Ayala, P. Y.; Morokuma, K.; Voth, G. A.; Salvador, P.; Dannenberg, J. J.; Zakrzewski, V. G.; Dapprich, S.; Daniels, A. D.; Strain, M. C.; Farkas, O.; Malick, D. K.; Rabuck, A. D.; Raghavachari, K.; Foresman, J. B.; Ortiz, J. V.; Cui, Q.; Baboul, A. G.; Clifford, S.; Cioslowski, J.; Stefanov, B. B.; Liu, G.; Liashenko, A.; Piskorz, P.; Komaromi, I.; Martin, R. L.; Fox, D. J.; Keith, T.; Al-Laham, M. A.; Peng, C. Y.; Nanayakkara, A.; Challacombe, M.; Gill, P. M. W.; Johnson, B.; Chen, W.; Wong, M. W.; Gonzalez, C.; Pople, J. A. *Gaussian 03*, Revision D.02; Gaussian, Inc.: Wallingford, CT, 2004. (b) Frisch, M. J.; Trucks, G. W.; Schlegel, H. B.; Scuseria, G. E.; Robb, M. A.; Cheeseman, J. R.; Scalmani, G.; Barone, V.; Mennucci, B.; Petersson, G. A.; Nakatsuji, H.; Caricato, M.; Li, X.; Hratchian, H. P.; Izmaylov, A. F.; Bloino, J.; Zheng, G.; Sonnenberg, J. L.; Hada, M.; Ehara, M.; Toyota, K.; Fukuda, R.; Hasegawa, J.; Ishida, M.; Nakajima, T.; Honda, Y.; Kitao, O.; Nakai, H.; Vreven, T.; Montgomery, J. A., Jr.; Peralta, J. E.; Ogliaro, F.; Bearpark, M.; Heyd, J. J.; Brothers, E.; Kudin, K. N.; Staroverov, V. N.; Kobayashi, R.; Normand, J.; Raghavachari, K.; Rendell, A.; Burant, J. C.; Iyengar, S. S.; Tomasi, J.; Cossi, M.; Rega, N.; Millam, J. M.; Klene, M.; Knox, J. E.; Cross, J. B.; Bakken, V.; Adamo, C.; Jaramillo, J.; Gomperts, R.; Stratmann, R. E.; Yazyev, O.; Austin, A. J.; Cammi, R.; Pomelli, C.; Ochterski, J. W.; Martin, R. L.; Morokuma, K.; Zakrzewski, V. G.; Voth, G. A.; Salvador, P.; Dannenberg, J. J.; Dapprich, S.; Daniels, A. D.; Farkas, Ö.; Foresman, J. B.; Ortiz, J. V.; Cioslowski, J.; Fox, D. J. *Gaussian 09*, Revision A.2; Gaussian, Inc.: Wallingford, CT, 2009.
- (26) Schmidt, M. W.; Baldrige, K. K.; Boatz, J. A.; Elbert, S. T.; Gordon, M. S.; Jensen, J. H.; Koseki, S.; Matsunaga, N.; Nguyen, K. A.; Su, S.; Windus, T. L.; Dupuis, M.; Montgomery, J. A., Jr. *J. Comput. Chem.* **1993**, *14*, 1347–1363.
- (27) (a) Hohenberg, P.; Kohn, W. *Phys. Rev.* **1964**, *136*, B864–871. (b) Kohn, W.; Sham, L. J. *Phys. Rev.* **1965**, *140*, A1133–1138.
- (28) (a) Becke, A. D. *Phys. Rev. A* **1988**, *38*, 3098–3100. (b) Becke, A. D. *J. Chem. Phys.* **1996**, *104*, 1040–1046.
- (29) For the assessment of the B1B95 and M06-2X functionals, see: (a) Riley, K. E.; Op't Holt, B. T.; Merz, K. M., Jr. *J. Chem. Theor. Comput.* **2007**, *3*, 407–433. (b) Pieniazek, S. N.; Clemente, F. R.; Houk, K. N. *Angew. Chem., Int. Ed.* **2008**, *47*, 7746–7749. (c) Plumley, J. A.; Evansck, J. D. *J. Chem. Theor. Comput.* **2008**, *4*, 1249–1253.
- (30) (a) Hehre, W. J.; Radom, L.; Schleyer, P. v. R.; Pople, J. A. *Ab Initio Molecular Orbital Theory*; Wiley: New York, 1986. For Br atom, see: (b) Binning, R. C., Jr.; Curtiss, L. A. *J. Comput. Chem.* **1990**, *11*, 1206–1216.
- (31) (a) Zhao, Y.; Truhlar, D. G. *Theor. Chem. Acc.* **2008**, *120*, 215–241. (b) Zhao, Y.; Truhlar, D. G. *Acc. Chem. Res.* **2008**, *41*, 157–167.
- (32) For the estimation of Gibbs free energy, the thermal correction term calculated at the B1B95/6-31G* level was used.
- (33) The electronic energy of TS-8XCS is higher than that of TS-6XCR by 0.6 kcal/mol at the M06-2X/6-311G**//M06-2X/6-311G* level, but the former is located lower than the latter by 1.4 kcal/mol at the MP2/6-311G**//M06-2X/6-311G* level.
- (34) At the M06-2X/6-311G**//B1B95/6-31G* level of theory, the transition-state structure corresponding to TS-1XTS is lower in Gibbs free energy than the structures which correspond to TS-6XCR, TS-6XTS, and TS-8XCS by 4.1, 5.1, and 5.5 kcal/mol, respectively, in the reaction catalyzed by the protonated oxazaborolidine cation.
- (35) (a) Fukui, K. *Acc. Chem. Res.* **1981**, *14*, 363–368. (b) Hratchian, H. P.; Schlegel, H. B. *J. Chem. Phys.* **2004**, *120*, 9918–9924.
- (36) (a) Jørgensen, K. A. In *Cycloaddition Reactions in Organic Synthesis*; Kobayashi, S., Jørgensen, K. A., Eds.; Wiley-VCH: Weinheim, 2002; p 301–327. (b) Ess, D. H.; Jones, G. O.; Houk, K. N. *Adv. Synth. Catal.* **2006**, *348*, 2337–2361. (c) Houk, K. N.; Strozier, R. W. *J. Am. Chem. Soc.* **1973**, *95*, 4094–4096. (d) Birney, D. M.; Houk, K. N. *J. Am. Chem. Soc.* **1990**, *112*, 4127–4133. (e) Yamabe, S.; Dai, T.; Minato, T. *J. Am. Chem. Soc.* **1995**, *117*, 10994–10997. (f) Dai, W.-M.; Lau, C. W.; Chung, S. H.; Wu, Y.-D. *J. Org. Chem.* **1995**, *60*, 8128–8129. (g) García, J. I.; Mayoral, J. A.; Salvatella, L. *J. Am. Chem. Soc.* **1996**, *118*, 11680–11681. (h) Ishihara, K.; Kondo, S.; Kurihara, H.; Yamamoto, H.; Ohashi, S.; Inagaki, S. *J. Org. Chem.* **1997**, *62*, 3026–3027. (i) García, J. I.; Martínez-Merino, V.; Mayoral, J. A.; Salvatella, L. *J. Am. Chem. Soc.* **1998**, *120*, 2415–2420. (j) Singleton, D. A.; Merrigan, S. R.; Beno, B. R.; Houk, K. N. *Tetrahedron Lett.* **1999**, *40*, 5817–5821. (k) Yamabe, S.; Minato, T. *J. Org. Chem.* **2000**, *65*, 1830–1841. (l) Avalos, M.; Babiano, R.; Bravo, J. L.; Cintas, P.; Jiménez, J. L.; Palacios, J. C.; Silva, M. A. *J. Org. Chem.* **2000**, *65*, 6613–6619. (m) Alves, C. N.; Carneiro, A. S.; Andrés, J.; Domingo, L. R. *Tetrahedron* **2006**, *62*, 5502–5509. (n) Berski, S.; Andrés, J.; Silvi, B.; Domingo, L. R. *J. Phys. Chem. A* **2006**, *110*, 13939–13947. (o) Sun, H.; Zhang, D.; Ma, C.; Liu, C. *Int. J. Quantum Chem.* **2007**, *107*, 1875–1885. (p) Xia, Y.; Yin, D.; Rong, C.; Xu, Q.; Yin, D.; Liu, S. *J. Phys. Chem. A* **2008**, *112*, 9970–9977. (q) Hayden, A. E.; DeChancie, J.; George, A. H.; Dai, M.; Yu, M.; Danishefsky, S. J.; Houk, K. N. *J. Org. Chem.* **2009**, *74*, 6770–6776.
- (37) Domingo, L. R.; Arnó, M.; Sáez, J. A. *J. Org. Chem.* **2009**, *74*, 5934–5940.
- (38) For the cycloaddition between cyclopentadiene and methacrolein catalyzed by AlBr₃, ΔE and ΔG^{195K} of the transition state relative to the initial state (C + M(*s-trans*) + AlBr₃) calculated at the M06-2X/6-311G**//B1B95/6-31G* level of theory are as follows: $\Delta E = -39.7$ (*s-cis* form, *endo* addition), -38.5 (*s-cis* form, *exo* addition), -37.7 (*s-trans* form, *endo* addition), and -38.4 (*s-trans* form, *exo* addition) kcal/mol. $\Delta G^{195K} = -20.7$ (*s-cis* form, *endo* addition), -18.9 (*s-cis* form, *exo* addition), -18.3 (*s-trans* form, *endo* addition), and -18.5 (*s-trans* form, *exo* addition) kcal/mol.
- (39) For the cycloaddition between cyclopentadiene and methacrolein catalyzed by AlBr₃, ΔG^{195K} of the transition state relative to the initial state (C + M(*s-trans*) + AlBr₃) calculated at the MP2/6-

311G**/B1B95/6-31G* level of theory are as follows: -19.9 (*s-cis* form, *endo* addition), -18.8 (*s-cis* form, *exo* addition), -20.6 (*s-trans* form, *endo* addition), and -20.0 (*s-trans* form, *exo* addition) kcal/mol.

(40) For the cycloaddition between cyclopentadiene and methacrolein without any catalyst, the energy and Gibbs free energy, ΔE and ΔG^{195K} , of the transition state relative to the initial state (C + M(*s-trans*)) calculated at the M06-2X/6-311G**/B1B95/6-31G* level of theory are as follows: $\Delta E = 12.0$ (*s-cis* form, *endo* addition), 10.8 (*s-cis* form, *exo* addition), 12.3 (*s-trans* form, *endo* addition), and 11.6 (*s-trans* form, *exo* addition) kcal/mol. $\Delta G^{195K} = 21.8$ (*s-cis* form, *endo* addition), 20.9 (*s-cis* form, *exo* addition), 22.8 (*s-trans* form, *endo* addition), and 21.8 (*s-trans* form, *exo* addition) kcal/mol.

(41) We found a complex between **2** and *s-trans* methacrolein, in which the distance between the oxygen atom of methacrolein and the boron atom of **2** is 3.132 \AA , and that between the hydrogen atom of methacrolein and the oxygen atom of **2** is 2.604 \AA . The stabilization comes mainly from a weak C–H \cdots O interaction (see the Supporting Information).

(42) De Vries, T. S.; Prokofjevs, A.; Vedejs, E. *Chem. Rev.* **2012**, *112*, 4246–4282.

(43) The ΔE is calculated at the CCSD(T)/6-311G**/B1B95/6-31G* level of theory to be -34.0 for **3N** and -35.8 kcal/mol for **3O**.

(44) (a) Fukui, K.; Koga, N.; Fujimoto, H. *J. Am. Chem. Soc.* **1981**, *103*, 196–197. (b) Fujimoto, H. *Acc. Chem. Res.* **1987**, *20*, 448–453.

(45) Reed, A. E.; Curtiss, L. A.; Weinhold, F. *Chem. Rev.* **1988**, *88*, 899–926.

(46) For population analysis along the reaction coordinate, see: Sakata, K. *J. Phys. Chem. A* **2000**, *104*, 10001–10008.

(47) Fujimoto, H.; Inagaki, H.; Fukui, K. *J. Am. Chem. Soc.* **1976**, *98*, 2670–2671.

(48) The natural population atomic charge of the C³ atom is -0.178 in (M·2·AlBr₃). It increases to -0.249 when AlBr₃ is removed, and to -0.301 when **2** is further removed, with the geometry of the remaining atoms frozen to the same as that in TS-8XCS. The corresponding atomic charge of the C² atom is -0.185 in (M·2·AlBr₃), -0.169 in (M·2), and -0.165 in M in the TS-8XCS structure.

(49) The antibonding overlap population arising from the repulsion is calculated to be -0.386 in total in the presence of **2n**, -0.388 in the presence of **2**, and -0.395 in the absence of the catalyst in the TS-8XCS structure. The part of the C¹(C)–C³(M) bond in the antibonding overlap population is -0.121 , -0.129 , and -0.146 , respectively.

(50) The Mulliken overlap population for the C¹(C)–C³(M) bond is 0.145 in TS-8XCS. It is reduced to 0.128 when AlBr₃ is removed, and to 0.088 in the absence of **2N**, with the geometry of the remaining atoms frozen to the same as that in TS-8XCS.

(51) In TS-6XCR, we also found the interaction between the B–C(*o*-tolyl) σ bond of **2** and a π^* orbital of M, in addition to electron donation from a lone-pair of electrons of **2** to the C–H σ^* orbital of M, i.e., the C–H \cdots O interaction (ref S2), suggested by Corey and co-workers.

(52) Corey, E. J.; Lee, T. W. *Chem. Commun.* **2001**, 1321–1329.

(53) (a) Fujimoto, H.; Mizutani, Y.; Iwase, K. *J. Phys. Chem.* **1986**, *90*, 2768–2772. (b) Fujimoto, H.; Satoh, S. *J. Phys. Chem.* **1994**, *98*, 1436–1441. (c) Fujimoto, H.; Sakata, K.; Fukui, K. *Int. J. Quantum Chem.* **1996**, *60*, 401–408. (d) Omoto, K.; Fujimoto, H. *J. Org. Chem.* **1998**, *63*, 8331–8336.

(54) The reference function δ_r was taken to be equiangular from the three bonds each connecting the boron atom and one of the adjacent atoms.

(55) (a) Corey, E. J.; Loh, T.-P. *J. Am. Chem. Soc.* **1991**, *113*, 8966–8967. (b) Corey, E. J. *Angew. Chem., Int. Ed.* **2002**, *41*, 1650–1667.

(56) Corey, E. J.; Yu, C.-M.; Kim, S. S. *J. Am. Chem. Soc.* **1989**, *111*, 5495–5496.

(57) Wong, M. W. *J. Org. Chem.* **2005**, *70*, 5487–5493.

(58) **2T'** is calculated to be more stable in energy than **2T** by 7.4 kcal/mol at the M06-2X/6-311G**/B1B95/6-31G* level of theory.